Available online at www.sciencedirect.com
SCIENCE DIRECT®
International Journal of Solids and Structures 42 (2005) 6032–6047
INTERNATIONAL JOURNAL OF SOLIDS and STRUCTURES
www.elsevier.com/locate/ijsolstr

Modeling of van der Waals force for infinitesimal deformation of multi-walled carbon nanotubes treated as cylindrical shells

Xiao Qiao He [a], Sritawat Kitipornchai [a,*], C.M. Wang [b], K.M. Liew [c]

[a] Department of Building and Construction, City University of Hong Kong, Tat Chee Avenue, Kowloon, Hong Kong, China
[b] Department of Civil Engineering, National University of Singapore, Kent Ridge, Singapore 119260, Singapore
[c] School of Mechanical and Production Engineering, Nanyang Technological University, Nanyang Avenue, Singapore 639798, Singapore

Received 4 March 2004

Abstract

This paper models van der Waals (vdW) force for axially compressed multi-walled carbon nanotubes (CNTs), whereby each tube is treated as a cylindrical shell continuum. Explicit formulas are derived for predicting the critical axial strain of a triple-walled CNT using a more refined vdW model. The analysis of a cylindrical shell continuum model of multi-walled CNTs using this refined vdW force model is carried out to study the influence of the effect of vdW interaction between different layers of a CNT and the size effect of a CNT on the vdW interaction. It is shown herein that the greatest contribution to the vdW interaction comes from the adjacent layers and the contribution from a remote layer may be neglected. The vdW interaction is found to be strongly dependent on the radius of the tube, especially when the radius is small enough (<7 nm). When the radius is large enough (>40 nm), the vdW interaction coefficient c_{ij} can be taken as a constant value (i.e. independent of radius). However, these constant values are different for the vdW interaction between two different layers of a multi-walled CNT. The effect of the vdW interaction on the critical axial strain of a triple-walled CNT for the cases of before and after buckling is also examined for various innermost radii.

Keywords: van der Waals interaction; Triple-walled carbon nanotube; Critical axial strain; Cylindrical shell model

* Corresponding author. Tel.: +852 27888028; fax: +852 27887612.
E-mail address: s.kitipornchai@cityu.edu.hk (S. Kitipornchai).

0020-7683/$ - see front matter
doi:10.1016/j.ijsolstr.2005.03.045

1. Introduction

Ever since their discovery in 1991 by Sumio Ijima of the NEC Laboratory in Tsukuba, Japan (Ijima, 1991), there has been intensive research into CNTs. This interest stems from the fact that CNTs have great potential applications as ropes to tether satellites, transistors in microcomputers, tubes for drug delivery, nanoprobes, etc. These applications draw on the remarkable mechanical and electrical properties of CNTs. They are as strong as diamonds and able to withstand bending and twisting better than steel. They can conduct electricity, act as semiconductors, and conduct heat rather well.

Single-walled CNTs are currently difficult to manufacture. They are usually produced in the form of multiple-walled tubes, with from three to more than a dozen tubes nested within one another. Due to the multi-walled nature of CNTs, there are forces between the carbon atoms that make up the cylindrical walls. These forces, called van der Waals forces, cannot be neglected because they are significant at this molecular scale.

Atomistic-based methods such as classical molecular dynamics (Ijima et al., 1996; Yakobson et al., 1997; Liew et al., 2004a,b), tight-binding molecular dynamics (Hernandez et al., 1998), and density functional theory (Sanchez-Portal et al., 1999) have been used to conduct rigorous bending, vibration, and buckling analyses of multi-walled CNTs. However, these methods require an enormous amount of computational time. Therefore, researchers have been diligently seeking more efficient computational methods with which to analyze multi-walled CNTs. Interestingly, it has been reported in the literature that continuum structural models, with which structural mechanists and engineers are familiar, may be applicable for the analysis of CNTs. In the last decade, many continuum structural models have been proposed. These include the beam model (e.g. Govindjee and Sackman, 1999; Yoon et al., 2003), the cylindrical shell model (e.g. Ru, 2000a,b,c, 2001a,b) and the space truss/frame model (e.g. Li and Chou, 2003a,b). One of the important aspects that all of these continuum models must possess is a good model for the vdW forces that exist at the molecular level in multi-walled CNTs. Ru (2001a) proposed a linear proportional relationship between the variation of the vdW and the normal deflection jump in modeling the vdW forces, but his model can only be applied to two adjacent layer interaction, as in the case of a double-walled CNT. For multi-walled CNTs, Ru's vdW model is not accurate because it neglects the effects of the other layers, except the adjacent layer, on the vdW interaction. It also does not consider the size effect (which is dependent on the radii of the tubes). The current practice in modeling the vdW forces in a continuum mechanics setting is to employ the so-called interaction constant c, the value of which is estimated by considering the interaction between a carbon atom and a flat graphite sheet (Kachanov, 1988). Using data from Saito et al. (2001), the interaction constant c has been calculated using this simple expression: $c = (320\,\text{ergs/cm}^2)/(0.16\bar{d}^2)$ where $\bar{d} = 0.142$ nm = the distance between the interacting atoms (Wang et al., 2003).

In this paper, we employ a more refined vdW model (He et al., 2005) for continuum structural models of multi-walled CNTs. The authors examined the vdW force interaction in axially compressed multi-walled CNTs that are approximated as cylindrical shell continuums. Explicit formulas for the critical axial strain of a triple-walled CNT are derived herein on the basis of a more refined vdW model. The validity of the proposed model is demonstrated by comparing it to existing results which were obtained by using an atomistic-based method.

2. Analytical formulation

Consider a multi-walled CNT that consists of two or more single CNTs of radius R_i, thickness h, and modulus of elasticity E. The tube is empty inside and no internal or external lateral pressures are applied to it except for the pressure caused by vdW interaction. We also assume that there is no sliding between layers.

Based on the classical thin shell theory (Timoshenko and Gere, 1961), the governing equations for the elastic buckling of a multi-walled CNT can be derived as the N coupled equations, i.e.

$$\begin{aligned} L_1 w_1 &= \nabla_1^4 p_1 \\ &\vdots \\ L_i w_i &= \nabla_i^4 p_i \\ &\vdots \\ L_N w_N &= \nabla_N^4 p_N \end{aligned} \tag{1}$$

where w_i $(i = 1, 2, \ldots, N)$ is the deflection of the ith tube, p_i is the pressure exerted on tube i due to the vdW interaction between walls, and L_i is the differential operator that is given by

$$L_i = D_i \nabla_i^8 - N_x \frac{\partial^2}{\partial x^2} \nabla_i^4 - \frac{N_\theta}{R_i^2} \frac{\partial^2}{\partial \theta^2} \nabla_i^4 + \frac{Eh}{R_i^2} \frac{\partial^4}{\partial x^4} \tag{2}$$

in which x and θ are the axial coordinate and the circumferential coordinate respectively, N_x and N_θ are the uniform axial and circumferential membrane forces of the ith tube prior to buckling, and D_i is the bending stiffness of the ith tube, and

$$\nabla_i^2 = \frac{\partial^2}{\partial x^2} + \frac{1}{R_i^2} \frac{\partial^2}{\partial \theta^2} \tag{3}$$

Due to the infinitesimal buckling jump (Ru, 2001a) of the deflection between two walls, the pressure due to vdW interaction can be expressed as

$$p_i(x, \theta) = -\sum_{j=1}^{i-1} p_{ij} + \sum_{j=i+1}^{N} p_{ij} + \sum_{j=1}^{N} \Delta p_{ij}(x, \theta) \tag{4}$$

where p_{ij} is the initial uniform vdW pressure contribution to the ith layer from the jth layer prior to buckling, N is the total number of layers of the multi-walled CNT, and Δp_{ij} is the pressure increment that is exerted on the ith layer from the jth layer, N is the total number of layers of the multi-walled CNT. As only infinitesimal buckling is considered, Δp_{ij} is assumed to be linearly proportional to the buckling deflection between two layers, i.e.

$$\Delta p_{ij} = c_{ij}(w_i - w_j) \tag{5}$$

where c_{ij} is the vdW interaction coefficient that will be determined in the sequel.

Finally, we obtain the following governing buckling equations for a multi-walled CNT.

$$\begin{aligned} L_1 w_1 &= \nabla_1^4 w_1 \sum_{j=1}^{N} c_{1j} - \sum_{j=1}^{N} c_{1j} \nabla_1^4 w_j \\ &\vdots \\ L_i w_i &= \nabla_i^4 w_i \sum_{j=1}^{N} c_{ij} - \sum_{j=1}^{N} c_{ij} \nabla_i^4 w_j \\ &\vdots \\ L_N w_N &= \nabla_N^4 w_N \sum_{j=1}^{N} c_{Nj} - \sum_{j=1}^{N} c_{Nj} \nabla_N^4 w_j \end{aligned} \tag{6}$$

These equations are coupled due to the vdW interaction.

3. vdW interaction

The vdW energy, due to the interatomic interaction, can be described by Lennard-Jones's pair potential V_{IJ} (Lennard-Jones, 1924; Girifalco and Lad, 1956; Girifalco, 1991)

$$V_{\mathrm{LJ}}(\bar{d}) = 4\varepsilon\left[\left(\frac{\sigma}{\bar{d}}\right)^{12} - \left(\frac{\sigma}{\bar{d}}\right)^{6}\right] \tag{7}$$

where $\bar{d}$ is the distance between the interacting atoms, ε is the depth of the potential, and σ is a parameter that is determined by the equilibrium distance. The vdW force F is obtained by taking the derivative of the Lennard-Jones pair potential, i.e.

$$F(\bar{d}) = -\frac{\mathrm{d}V_{\mathrm{LJ}}(\bar{d})}{\mathrm{d}\bar{d}} = \frac{24\varepsilon}{\sigma}\left[2\left(\frac{\sigma}{\bar{d}}\right)^{13} - \left(\frac{\sigma}{\bar{d}}\right)^{7}\right] \tag{8}$$

The Lennard-Jones model provides a smooth transition between (a) the attractive force of an approaching pair of atoms from a certain distance and (b) the repulsive force when the distance of the interacting atoms becomes less than the sum of their contact radii.

It should be noted that we are only interested in the infinitesimal buckling of a CNT. Thus, the vdW force can be estimated by the Taylor expansion to the first-order around the equilibrium position prior to buckling, i.e.

$$\begin{aligned} F(\bar{d}) &= F(\bar{d}_0) + \frac{\mathrm{d}F(\bar{d}_0)}{\mathrm{d}\bar{d}}(\bar{d} - \bar{d}_0) \\ &= \frac{24\varepsilon}{\sigma}\left[2\left(\frac{\sigma}{\bar{d}_0}\right)^{13} - \left(\frac{\sigma}{\bar{d}_0}\right)^{7}\right] - \frac{24\varepsilon}{\sigma^2}\left[26\left(\frac{\sigma}{\bar{d}_0}\right)^{14} - 7\left(\frac{\sigma}{\bar{d}_0}\right)^{8}\right](\bar{d} - \bar{d}_0) \end{aligned} \tag{9}$$

where $\bar{d}_0 = \sqrt{(R_j\cos\theta - R_i)^2 + R_j^2\sin^2\theta + x^2}$ is the initial interlayer separation prior to buckling.

The vdW force exerted on any atom on a tube can be estimated by summing all forces between the atom and all atoms on the other tube. To simplify the calculations, we consider the CNT as a continuum cylindrical shell and note that each carbon atom corresponds to the area of $9a^2/4\sqrt{3}$ (Saito et al., 1998). Thus, the integration of Eq. (9) over the entire CNT leads to an analytical representation for the initial pressure p_{ij} caused by the vdW interaction:

$$\begin{aligned} p_{ij} &= \left(\frac{4\sqrt{3}}{9a^2}\right)^2 \frac{24\varepsilon}{\sigma}\int_{-\pi}^{\pi}\int_{-L/2}^{L/2}\left[2\left(\frac{\sigma}{\bar{d}_0}\right)^{13} - \left(\frac{\sigma}{\bar{d}_0}\right)^{7}\right]R_j\,\mathrm{d}x\,\mathrm{d}\theta \\ &= \left[\frac{2048\varepsilon\sigma^{12}}{9a^4}\sum_{k=0}^{5}\frac{(-1)^k}{2k+1}\binom{5}{k}E_{ij}^{12} - \frac{1024\varepsilon\sigma^6}{9a^4}\sum_{k=0}^{2}\frac{(-1)^k}{2k+1}\binom{2}{k}E_{ij}^{6}\right]R_j \end{aligned} \tag{10}$$

where $a = 1.42$ Å is the C–C bond length, R_j is the radius of the jth layer, and the subscripts i and j denote the ith and jth layers, respectively. The pressure increment due to the buckling jump is given by

$$\begin{aligned} \Delta p_{ij} &= -\left(\frac{4\sqrt{3}}{9a^2}\right)^2 \frac{24\varepsilon}{\sigma^2}\int_{-\pi}^{\pi}\int_{-L/2}^{L/2}\left[26\left(\frac{\sigma}{\bar{d}_0}\right)^{14} - 7\left(\frac{\sigma}{\bar{d}_0}\right)^{8}\right](\bar{d} - \bar{d}_0)R_j\,\mathrm{d}x\,\mathrm{d}\theta \\ &= -\left[\frac{1001\pi\varepsilon\sigma^{12}}{3a^4}E_{ij}^{13} - \frac{1120\pi\varepsilon\sigma^6}{9a^4}E_{ij}^{7}\right]R_j(w_i - w_j) \end{aligned} \tag{11}$$

where E_{ij}^6, E_{ij}^7, E_{ij}^{12} and E_{ij}^{13} are the elliptical integrals defined by

$$E_{ij}^m = \left(R_j + R_i\right)^{-m} \int_0^{\pi/2} \frac{d\theta}{\left[1 - K_{ij}\cos^2\theta\right]^{m/2}} \tag{12}$$

where m is an integer and

$$K_{ij} = \frac{4R_jR_i}{\left(R_j + R_i\right)^2} \tag{13}$$

Comparing Eqs. (5) and (11) we have

$$c_{ij} = -\left[\frac{1001\pi\varepsilon\sigma^{12}}{3a^4}E_{ij}^{13} - \frac{1120\pi\varepsilon\sigma^6}{9a^4}E_{ij}^7\right]R_j \tag{14}$$

Eq. (14) furnishes the mathematical expression for the interaction coefficient c_{ij} that models the vdW forces in a multi-walled CNT, where each tube has been treated as an individual cylindrical shell continuum. This more refined vdW model captures the effects of all layers, not just those between two adjacent layers. For example, $c\,(4,3)$ furnishes the effect of vdW force on layer 4 by layer 3, and $c\,(4,2)$ furnishes the effect of vdW force on layer 4 by layer 2. Moreover, the expression accounts for the size effect.

4. The critical axial strain of a triple-walled CNT

Consider an axially compressed multi-walled CNT, in which the individual tube is treated as a cylindrical shell of radius R_i, thickness h, and Young's modulus E, as shown in Fig. 1. Each tube is referred to a coordinate system (x,θ). Here, x and θ are axial coordinate and circumferential angular coordinate, respectively. No internal or external lateral pressures are applied to the innermost tube or outermost tube except for the pressure caused by vdW interaction. The ends of all the three tubes are assumed to be simply supported. Thus, the buckling modes of all the tubes can be approximate as

$$w_k = A_k \sin\frac{m\pi x}{L}\cos n\theta \tag{15}$$

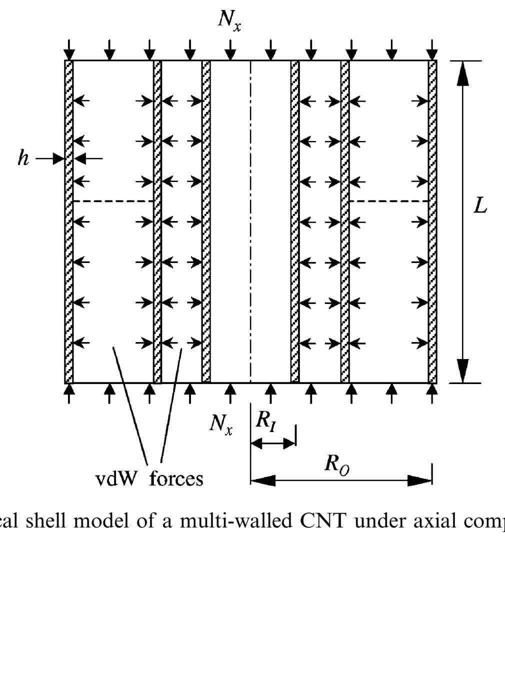

Fig. 1. A continuum cylindrical shell model of a multi-walled CNT under axial compression and vdW interaction.

where A_k ($k = 1, 2, \ldots, N$) are unknown coefficients, L is the length of the multi-walled CNT, m is the axial half wavenumber and n the circumferential wavenumber.

The substitution of Eq. (15) into Eq. (6) leads to a set of equations with N unknowns of A_k ($k = 1, 2, \ldots, N$). The equation for determining the critical axial strain of a multi-walled CNT is obtained by setting the determinant of $A_1, A_2, \ldots$ and A_N to zero, i.e.

$$\det\left(-[\mathbf{H}] - N_x\left(\frac{m\pi}{L}\right)^2[\mathbf{I}]\right) = 0 \tag{16}$$

where $\mathbf{I}$ is an identity matrix and the elements in the matrix $\mathbf{H}$ are

$$h_{ij} = c_{ij}, \quad i \neq j \tag{17}$$

and

$$h_{kk} = D\left[\left(\frac{m\pi}{L}\right)^2 + \left(\frac{n}{R_k}\right)^2\right]^2 - \sum_{\substack{j=1 \\ j\neq k}}^{N} c_{kj} - p_k R_k \left(\frac{n}{R_k}\right)^2 + \frac{Eh}{R_k^2}\left[\frac{1}{1 + \left(\frac{Ln}{m\pi R_k}\right)^2}\right]^2 \tag{18}$$

where $p_k = -N_\theta/R_k$ ($k = 1, 2, \ldots, N$) is the net pressure exerted on kth tube, which is assumed to be inward. Thus, the buckling axial strain relative to the wavenumber of m and n is determined by solving Eq. (16).

For a triple-walled CNT, Eq. (16) can be reduced to the following equation

$$N_x^3\left(\frac{m\pi}{L}\right)^6 + a_1 N_x^2\left(\frac{m\pi}{L}\right)^4 + a_2 N_x\left(\frac{m\pi}{L}\right)^2 + a_3 = 0 \tag{19}$$

where

$$\begin{aligned} a_1 &= h_{11} + h_{22} + h_{33} \\ a_2 &= h_{11}h_{22} + h_{11}h_{33} + h_{22}h_{33} - c_{31}c_{13} - c_{21}c_{12} - c_{23}c_{32} \\ a_3 &= h_{11}h_{22}h_{33} - h_{22}c_{31}c_{13} - h_{33}c_{21}c_{12} - h_{11}c_{23}c_{32} + c_{21}c_{32}c_{13} + c_{31}c_{23}c_{12} \end{aligned} \tag{20a–c}$$

The buckling axial strain can be obtained by solving Eq. (19) as follows:

$$-\frac{N_k}{Eh} = -\frac{L^2}{Ehm^2\pi^2}\left(\frac{2}{3}\sqrt{a_1^2 - 3a_2}\cos\frac{\alpha + (k-1)\times 2\pi}{3} + \frac{a_1}{3}\right), \quad k = 1, 2 \text{ and } 3 \tag{21}$$

where

$$\alpha = \cos^{-1}\frac{27a_3 + 2a_1^3 - 9a_1a_2}{2\sqrt{(a_1^2 - 3a_2)^3}} \tag{22}$$

The critical axial strain is thus the lowest buckling strain determined by Eq. (21) with respective to every combination of the integer m and n.

5. Numerical results and discussion

This section presents numerical results for the vdW interaction of multi-walled CNT with various dimensions. Consider a multi-walled CNT with an innermost radius R_I and an outermost radius R_O, as shown in Fig. 1. We assume that each tube has the same length L and thickness h, and is modeled as an individual cylindrical shell. The CNT is subjected to the combined action of axial compression and vdW interaction. Following most published papers on CNTs, the initial interlayer separation between the two adjacent layers is assumed to be 0.34 nm.

To illustrate the explicit expressions for the vdW interaction (prior to buckling), a 10-walled CNT with innermost radius $R_I = 0.68$ nm is considered. The parameters used in the vdW potential (given by Eq. (7)) are taken as $\varepsilon = 2.968$ meV and $\sigma = 3.407$ Å (these values used by Saito et al., 2001). The initial vdW pressure is calculated using Eq. (10) for each layer of the 10-walled CNT. Table 1 shows the initial vdW pressures p_{ij} before buckling. Here i and j vary from the innermost layer 1 to outermost layer 10. It should be noted that the negative sign represents an attraction between two layers. From the results presented in Table 1, it can be seen that the initial pressure between two adjacent layers is much larger than the other two layers, and the pressure decreases monotonically with increasing distance between two layers until it reaches zero or is negligible when the distance is large enough.

To illustrate the vdW interaction (after buckling), the vdW interaction coefficient c_{ij} is calculated using Eq. (14) for each layer of the 10-walled CNT. The vdW interaction coefficients c_{ij} are shown in Table 2. The values of the coefficients in Table 2 represent the vdW pressure contribution to layer i from layer j due to the jump of the buckling deflection. It can be observed from Table 2 that the vdW interaction between two adjacent layers is much larger than that between the other two layers, and the coefficient decreases rapidly from the adjacent layer to the innermost or outermost layers. Thus, when the difference between the numbers of the two layers is large enough, the value of the coefficient is very small compared to the net pressure, and the vdW interaction can be neglected. The coefficients between two adjacent layers are compared with the results that were obtained by Wang et al. (2003) for various layers, as shown in Table 2. Note that Wang's vdW force model only takes into consideration the vdW interaction between two adjacent layers, and the interaction coefficient c is assumed to be a constant. As shown in Table 2, the present results (based on the newly proposed vdW force model) are about 10% higher than Wang's results. However, the value of the percentage differences in the coefficient values depends on the radius of the tubes in a multi-walled CNT.

To investigate the dimension effect, the coefficients c_{1j} and c_{5j} ($j = 1$–10 for the 10 layers) are calculated using Eq. (14) for various values of innermost radius R_I of a 10-walled CNT. The results are presented in Tables 3 and 4. As can be seen, the innermost radius affects the coefficients because the surface area of the tube varies with respect to the radius, and the force that is exerted on each carbon atom of the surface is the sum of the vdW forces from all atoms on the other surface. Thus, the vdW pressure varies with the different radii of tubes. Similarly, Tables 5 and 6 show the initial vdW pressures p_{1j} and p_{5j}. The initial pressures are also different for varying radii of the tubes.

To show the relationship between vdW pressure and the radius of a tube, we consider the effect of other layers on the fourth layer. Again using Eq. (14), the values of the vdW interaction coefficients c_{43} and c_{45}, c_{42} and c_{46}, and c_{41} and c_{47} are calculated and plotted in Fig. 2a–c for various radii of the 4th layer of a multi-walled CNT. It can be seen from Fig. 2a–c that the coefficient decreases rapidly with increasing radius of the 4th layer until the radius reaches 7 nm. After passing this radius value, the coefficient decreases slowly until it approaches the constant values of −108 and −109 GPa/nm for c_{43} and c_{45} respectively, the constant values of 1.84 and 1.91 GPa/nm for c_{42} and c_{46}, respectively, and the constant values of 0.167 and 0.171 GPa/nm for c_{41} and c_{47}, respectively.

The greatest influence on the initial vdW pressure of the fourth layer prior to buckling comes from p_{43} and p_{45} (two adjacent layers), p_{42} and p_{46}, andp_{41} and p_{47}. The pressure from the inside layer is inward while the pressure from the outside is outward. Fig. 3a–c show the absolute values of the initial vdW pressure contributions to the fourth layer from two side layers for various radii of the tubes. As can be seen from Fig. 3a–c, the size of the radius only significantly affects the initial pressure for small radius, such as a radius of less than 7 nm, and has little influence on the pressure for a larger radius. Once again, the pressure approaches a constant value as the radius increases. The constants are 571 and 575 MPa for p_{43} and p_{45} respectively, 220 and 223 MPa for p_{42} and p_{46} respectively, and 29 and 30 MPa for p_{41} and p_{47} respectively.

Fig. 4 shows the initial net pressure on each layer of a 10-walled CNT due to the vdW forces before buckling for various innermost radii R_I. Most of the layers are exposed to an outward net pressure except

Table 1
Initial pressure p_{ij} (MPa) due to vdW interaction between tubes i and j for a 10-walled CNT with innermost radius $R_I = 0.68$ nm

Number of layers, N	$j = 1$	$j = 2$	$j = 3$	$j = 4$	$j = 5$	$j = 6$	$j = 7$	$j = 8$	$j = 9$	$j = 10$
$i = 1$	0.0000E+00	−0.7486E+03	−0.3211E+03	−0.4843E+02	−0.1295E+02	−0.4659E+01	−0.2028E+01	−0.1005E+01	−0.5467E+00	−0.3195E+00
$i = 2$	−0.4991E+03	0.0000E+00	−0.6827E+03	−0.2897E+03	−0.4284E+02	−0.1114E+02	−0.3953E+01	−0.1706E+01	−0.8412E+00	−0.4569E+00
$i = 3$	−0.1605E+03	−0.5120E+03	0.0000E+00	−0.6525E+03	−0.2735E+03	−0.3971E+02	−0.1018E+02	−0.3572E+01	−0.1528E+01	−0.7488E+00
$i = 4$	−0.1954E+02	−0.1738E+03	−0.5220E+03	0.0000E+00	−0.6353E+03	−0.2635E+03	−0.3779E+02	−0.9583E+01	−0.3335E+01	−0.1417E+01
$i = 5$	−0.4317E+01	−0.2142E+02	−0.1823E+03	−0.5294E+03	0.0000E+00	−0.6242E+03	−0.2568E+03	−0.3649E+02	−0.9181E+01	−0.3173E+01
$i = 6$	−0.1331E+01	−0.4772E+01	−0.2269E+02	−0.1882E+03	−0.5350E+03	0.0000E+00	−0.6164E+03	−0.2520E+03	−0.3555E+02	−0.8889E+01
$i = 7$	−0.5069E+00	−0.1482E+01	−0.5088E+01	−0.2362E+02	−0.1926E+03	−0.5394E+03	0.0000E+00	−0.6107E+03	−0.2483E+03	−0.3483E+02
$i = 8$	−0.2232E+00	−0.5686E+00	−0.1587E+01	−0.5324E+01	−0.2433E+02	−0.1960E+03	−0.5428E+03	0.0000E+00	−0.6063E+03	−0.2454E+03
$i = 9$	−0.1093E+00	−0.2524E+00	−0.6113E+00	−0.1667E+01	−0.5509E+01	−0.2488E+02	−0.1986E+03	−0.5457E+03	0.0000E+00	−0.6028E+03
$i = 10$	−0.5808E−01	−0.1246E+00	−0.2723E+00	−0.6439E+00	−0.1731E+01	−0.5657E+01	−0.2533E+02	−0.2008E+03	−0.5480E+03	0.0000E+00

Table 2
vdW interaction coefficients c_{ij} (GPa/nm) between tubes i and j for a 10-walled CNT with innermost radius $R_{\mathrm{I}} = 0.68$ nm

Number of layers, N	$j = 1$	$j = 2$	$j = 3$	$j = 4$	$j = 5$	$j = 6$	$j = 7$	$j = 8$	$j = 9$	$j = 10$
$i = 1$	0.0000E+00	−0.1328E+03 −0.9919E+02[a]	0.2696E+01	0.2762E+00	0.5489E−01	0.1580E−01	0.5737E−02	0.2442E−02	0.1166E−02	0.6078E−03
$i = 2$	−0.8856E+02	0.0000E+00	−0.1254E+03 −0.9919E+02[a]	0.2439E+01	0.2431E+00	0.4733E−01	0.1342E−01	0.4821E−02	0.2037E−02	0.9687E−03
$i = 3$	0.1348E+01	−0.9402E+02	0.0000E+00	−0.1214E+03 −0.9919E+02[a]	0.2306E+01	0.2259E+00	0.4336E−01	0.1215E−01	0.4327E−02	0.1815E−02
$i = 4$	0.1105E+00	0.1463E+01	−0.9714E+02	0.0000E+00	−0.1190E+03 −0.9919E+02[a]	0.2223E+01	0.2152E+00	0.4091E−01	0.1137E−01	0.4019E−02
$i = 5$	0.1830E−01	0.1216E+00	0.1537E+01	−0.9915E+02	0.0000E+00	−0.1173E+03 −0.9919E+02[a]	0.2168E+01	0.2080E+00	0.3924E−01	0.1084E−01
$i = 6$	0.4514E−02	0.2028E−01	0.1291E+00	0.1588E+01	−0.1006E+03	0.0000E+00	−0.1161E+03 −0.9919E+02[a]	0.2127E+01	0.2027E+00	0.3802E−01
$i = 7$	0.1434E−02	0.5031E−02	0.2168E−01	0.1345E+00	0.1626E+01	−0.1016E+03	0.0000E+00	−0.1152E+03 −0.9919E+02[a]	0.2096E+01	0.1987E+00
$i = 8$	0.5427E−03	0.1607E−02	0.5402E−02	0.2273E−01	0.1387E+00	0.1654E+01	−0.1024E+03	0.0000E+00	−0.1145E+03 −0.9919E+02[a]	0.2072E+01
$i = 9$	0.2333E−03	0.6112E−03	0.1731E−02	0.5686E−02	0.2354E−01	0.1419E+00	0.1677E+01	−0.1031E+03	0.0000E+00	−0.1139E+03 −0.9919E+02[a]
$i = 10$	0.1105E−03	0.2642E−03	0.6600E−03	0.1827E−02	0.5911E−02	0.2420E−01	0.1445E+00	0.1696E+01	−0.1036E+03	0.0000E+00

[a] Results obtained from Wang et al. (2003).

Table 3
vdW interaction coefficients c_{1j} (GPa/nm) for a 10-walled CNT for various innermost radii R_I

R_I (nm)	$j=1$	$j=2$	$j=3$	$j=4$	$j=5$	$j=6$	$j=7$	$j=8$	$j=9$	$j=10$
0.68	0.0000E+00	−0.1328E+03	0.2696E+01	0.2762E+00	0.5489E−01	0.1580E−01	0.5737E−02	0.2442E−02	0.1166E−02	0.6078E−03
1.36	0.0000E+00	−0.1214E+03	0.2306E+01	0.2259E+00	0.4336E−01	0.1215E−01	0.4327E−02	0.1815E−02	0.8580E−03	0.4441E−03
2.04	0.0000E+00	−0.1173E+03	0.2168E+01	0.2080E+00	0.3924E−01	0.1084E−01	0.3809E−02	0.1580E−02	0.7398E−03	0.3798E−03
2.72	0.0000E+00	−0.1152E+03	0.2096E+01	0.1987E+00	0.3709E−01	0.1015E−01	0.3538E−02	0.1457E−02	0.6779E−03	0.3460E−03
3.40	0.0000E+00	−0.1139E+03	0.2053E+01	0.1930E+00	0.3577E−01	0.9727E−02	0.3372E−02	0.1381E−02	0.6395E−03	0.3250E−03
4.08	0.0000E+00	−0.1131E+03	0.2024E+01	0.1891E+00	0.3488E−01	0.9439E−02	0.3258E−02	0.1330E−02	0.6134E−03	0.3107E−03
4.76	0.0000E+00	−0.1125E+03	0.2002E+01	0.1863E+00	0.3422E−01	0.9230E−02	0.3175E−02	0.1292E−02	0.5944E−03	0.3002E−03
5.44	0.0000E+00	−0.1120E+03	0.1987E+01	0.1842E+00	0.3373E−01	0.9071E−02	0.3112E−02	0.1263E−02	0.5799E−03	0.2923E−03
6.12	0.0000E+00	−0.1116E+03	0.1974E+01	0.1826E+00	0.3334E−01	0.8946E−02	0.3063E−02	0.1241E−02	0.5684E−03	0.2860E−03
6.80	0.0000E+00	−0.1113E+03	0.1964E+01	0.1812E+00	0.3303E−01	0.8845E−02	0.3023E−02	0.1223E−02	0.5592E−03	0.2810E−03

Table 4
vdW interaction coefficients c_{5j} (GPa/nm) between tubes i and j for a 10-walled CNT for various innermost radii R_I

R_I (nm)	$j=1$	$j=2$	$j=3$	$j=4$	$j=5$	$j=6$	$j=7$	$j=8$	$j=9$	$j=10$
0.68	0.1830E−01	0.1216E+00	0.1537E+01	−0.9915E+02	0.0000E+00	−0.1173E+03	0.2168E+01	0.2080E+00	0.3924E−01	0.1084E−01
1.36	0.2168E−01	0.1345E+00	0.1626E+01	−0.1016E+03	0.0000E+00	−0.1152E+03	0.2096E+01	0.1987E+00	0.3709E−01	0.1015E−01
2.04	0.2354E−01	0.1419E+00	0.1677E+01	−0.1031E+03	0.0000E+00	−0.1139E+03	0.2053E+01	0.1930E+00	0.3577E−01	0.9727E−02
2.72	0.2473E−01	0.1467E+00	0.1711E+01	−0.1040E+03	0.0000E+00	−0.1131E+03	0.2024E+01	0.1891E+00	0.3488E−01	0.9439E−02
3.40	0.2555E−01	0.1500E+00	0.1735E+01	−0.1047E+03	0.0000E+00	−0.1125E+03	0.2002E+01	0.1863E+00	0.3422E−01	0.9230E−02
4.08	0.2616E−01	0.1524E+00	0.1752E+01	−0.1052E+03	0.0000E+00	−0.1120E+03	0.1987E+01	0.1842E+00	0.3373E−01	0.9071E−02
4.76	0.2662E−01	0.1543E+00	0.1766E+01	−0.1056E+03	0.0000E+00	−0.1116E+03	0.1974E+01	0.1826E+00	0.3334E−01	0.8946E−02
5.44	0.2699E−01	0.1558E+00	0.1777E+01	−0.1059E+03	0.0000E+00	−0.1113E+03	0.1964E+01	0.1812E+00	0.3303E−01	0.8845E−02
6.12	0.2728E−01	0.1571E+00	0.1785E+01	−0.1062E+03	0.0000E+00	−0.1111E+03	0.1956E+01	0.1801E+00	0.3278E−01	0.8762E−02
6.80	0.2753E−01	0.1581E+00	0.1793E+01	−0.1064E+03	0.0000E+00	−0.1109E+03	0.1949E+01	0.1792E+00	0.3256E−01	0.8693E−02

Table 5
Initial pressure p_{1j} (MPa) due to vdW interaction for a 10-walled CNT for various innermost radii R_I

R_I (nm)	$j=1$	$j=2$	$j=3$	$j=4$	$j=5$	$j=6$	$j=7$	$j=8$	$j=9$	$j=10$
0.68	0.0000E+00	−0.7486E+03	−0.3211E+03	−0.4843E+02	−0.1295E+02	−0.4659E+01	−0.2028E+01	−0.1004E+01	−0.5467E+00	−0.3194E+00
1.36	0.0000E+00	−0.6525E+03	−0.2735E+03	−0.3971E+02	−0.1018E+02	−0.3572E+01	−0.1528E+01	−0.7488E+00	−0.4048E+00	−0.2358E+00
2.04	0.0000E+00	−0.6242E+03	−0.2568E+03	−0.3649E+02	−0.9181E+01	−0.3173E+01	−0.1340E+01	−0.6496E+00	−0.3480E+00	−0.2012E+00
2.72	0.0000E+00	−0.6107E+03	−0.2483E+03	−0.3483E+02	−0.8668E+01	−0.2967E+01	−0.1242E+01	−0.5976E+00	−0.3181E+00	−0.1828E+00
3.40	0.0000E+00	−0.6028E+03	−0.2431E+03	−0.3382E+02	−0.8353E+01	−0.2841E+01	−0.1182E+01	−0.5656E+00	−0.2995E+00	−0.1714E+00
4.08	0.0000E+00	−0.5976E+03	−0.2396E+03	−0.3313E+02	−0.8141E+01	−0.2755E+01	−0.1142E+01	−0.5439E+00	−0.2870E+00	−0.1636E+00
4.76	0.0000E+00	−0.5940E+03	−0.2371E+03	−0.3264E+02	−0.7987E+01	−0.2693E+01	−0.1112E+01	−0.5282E+00	−0.2778E+00	−0.1580E+00
5.44	0.0000E+00	−0.5913E+03	−0.2352E+03	−0.3226E+02	−0.7870E+01	−0.2646E+01	−0.1090E+01	−0.5163E+00	−0.2709E+00	−0.1537E+00
6.12	0.0000E+00	−0.5892E+03	−0.2337E+03	−0.3197E+02	−0.7779E+01	−0.2609E+01	−0.1072E+01	−0.5069E+00	−0.2655E+00	−0.1503E+00
6.80	0.0000E+00	−0.5875E+03	−0.2325E+03	−0.3174E+02	−0.7706E+01	−0.2579E+01	−0.1058E+01	−0.4993E+00	−0.2611E+00	−0.1476E+00

Table 6
Initial pressure p_{5j}(MPa) due to vdW interaction for a 10-walled CNT for various innermost radii R_I

R_I(nm)	$j=1$	$j=2$	$j=3$	$j=4$	$j=5$	$j=6$	$j=7$	$j=8$	$j=9$	$j=10$
0.68	−0.4317E+01	−0.2142E+02	−0.1823E+03	−0.5294E+03	0.0000E+00	−0.6242E+03	−0.2568E+03	−0.3649E+02	−0.9181E+01	−0.3173E+01
1.36	−0.5088E+01	−0.2362E+02	−0.1926E+03	−0.5394E+03	0.0000E+00	−0.6107E+03	−0.2483E+03	−0.3483E+02	−0.8668E+01	−0.2967E+01
2.04	−0.5508E+01	−0.2488E+02	−0.1986E+03	−0.5457E+03	0.0000E+00	−0.6028E+03	−0.2431E+03	−0.3382E+02	−0.8353E+01	−0.2841E+01
2.72	−0.5778E+01	−0.2570E+02	−0.2026E+03	−0.5500E+03	0.0000E+00	−0.5976E+03	−0.2396E+03	−0.3313E+02	−0.8141E+01	−0.2755E+01
3.40	−0.5967E+01	−0.2628E+02	−0.2054E+03	−0.5531E+03	0.0000E+00	−0.5940E+03	−0.2371E+03	−0.3264E+02	−0.7987E+01	−0.2693E+01
4.08	−0.6105E+01	−0.2670E+02	−0.2074E+03	−0.5555E+03	0.0000E+00	−0.5913E+03	−0.2352E+03	−0.3226E+02	−0.7870E+01	−0.2646E+01
4.76	−0.6212E+01	−0.2703E+02	−0.2091E+03	−0.5574E+03	0.0000E+00	−0.5892E+03	−0.2337E+03	−0.3197E+02	−0.7779E+01	−0.2609E+01
5.44	−0.6296E+01	−0.2729E+02	−0.2103E+03	−0.5589E+03	0.0000E+00	−0.5875E+03	−0.2325E+03	−0.3174E+02	−0.7706E+01	−0.2579E+01
6.12	−0.6365E+01	−0.2751E+02	−0.2114E+03	−0.5601E+03	0.0000E+00	−0.5861E+03	−0.2315E+03	−0.3154E+02	−0.7645E+01	−0.2555E+01
6.80	−0.6422E+01	−0.2768E+02	−0.2122E+03	−0.5612E+03	0.0000E+00	−0.5850E+03	−0.2307E+03	−0.3138E+02	−0.7595E+01	−0.2535E+01

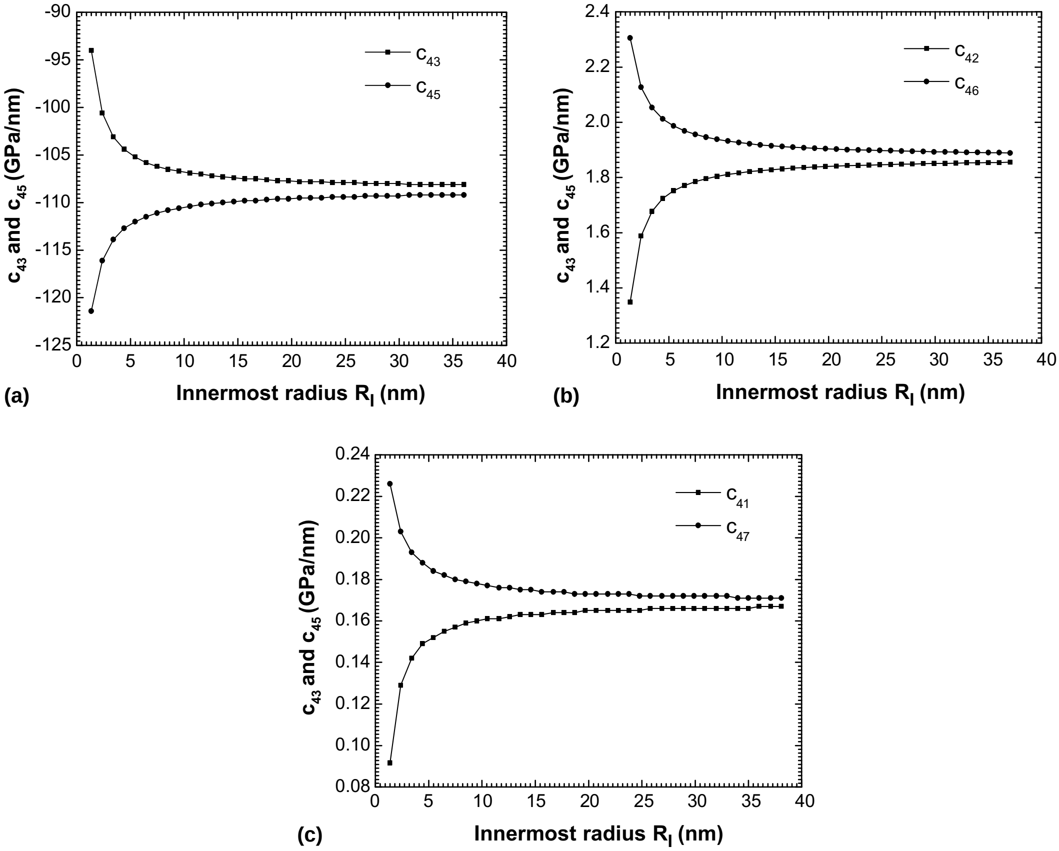

Fig. 2. (a)–(c) vdW interaction coefficients versus the radius of the 4th layer of a multi-walled CNT.

for the outermost two layers, which are exposed to an inward pressure. The initial net pressures that are exerted on the innermost two layers and outermost two layers are much larger than those on the other layers. For the intermediate layers, the net pressures are close to zero because the vdW interactions from two sides counteract each other.

To validate the proposed buckling model, we consider a multi-walled CNT of innermost radius $R_I = 0.34$ nm, as shown in Fig. 1. The bending stiffness $D = 0.85$ eV, $Eh = 360$ J/m^2 (Yakobson et al., 1996), and the length to the outermost radius ratio $L/R_O = 10$ are adopted. Fig. 5 shows the critical axial strains of multi-walled CNTs with layers varying from 2 to 10. As can be seen, the critical axial strain decreases with the increase of layers. For the double-, triple- and four-walled CNTs, the critical axial strains obtained from the present model are compared with the results obtained from MD simulation by Liew et al. (2004b). It is observed from Fig. 5 that results obtained by the present model are in good agreement with those of Liew et al. (2004b), and the relative errors for the critical axial strain of double-, triple- and four-walled CNTs are 0.16%, 13.4% and 15%, respectively. We noted that Yakobson et al. (1996) obtained a critical axial strain, i.e. $\varepsilon_1 = 0.05$ for a single-walled CNT of radius $R = 0.477$ nm by using the MD simulation. This value of the critical strain is also close to our calculated critical strain $\varepsilon_c = 0.0599$ for the double-walled CNT with outermost radius $R_O = 0.68$ nm, as shown in Fig. 5.

Having validated the present model, the critical axial strain for the triple-walled CNT has been investigated for various innermost radii R_I, as shown in Fig. 6. For a triple-walled CNT with small radius, say the

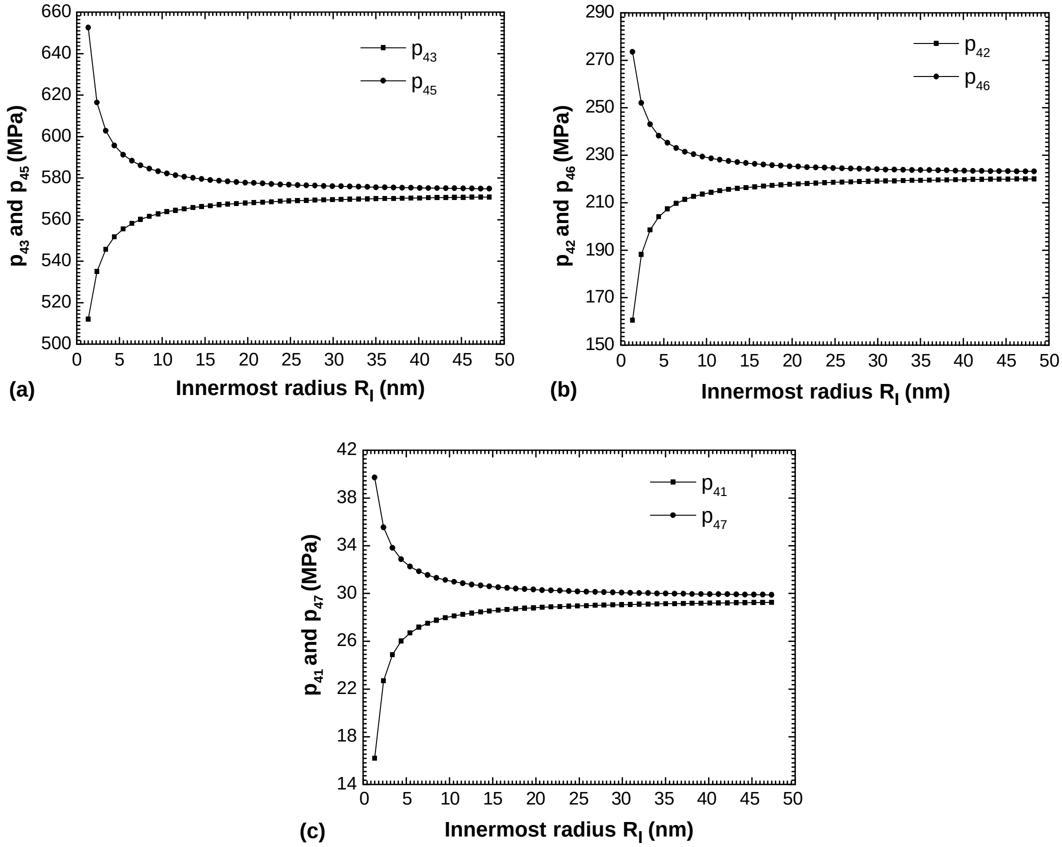

Fig. 3. (a)–(c) Initial vdW pressure versus the radius of the 4th layer of a multi-walled CNT.

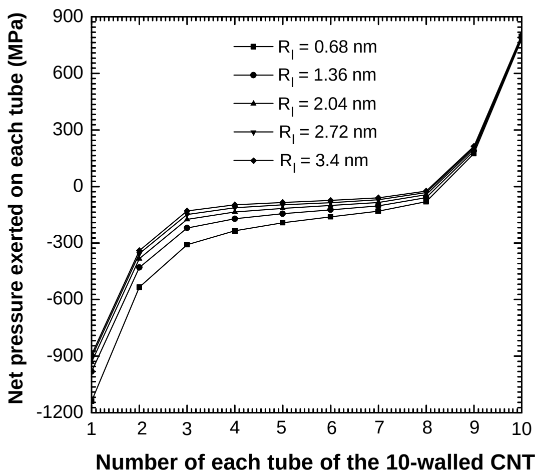

Fig. 4. Initial net pressures on each tube of a 10-walled CNT with various innermost radii R_I.

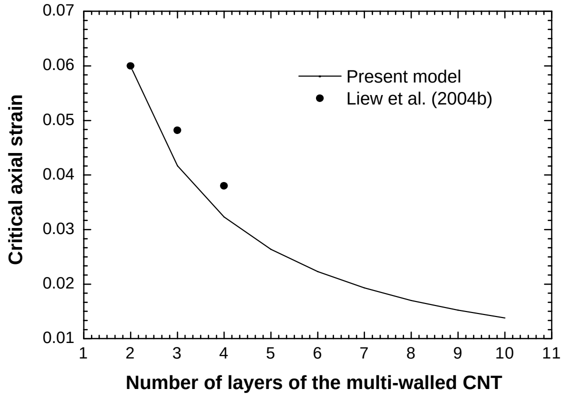

Fig. 5. Comparison of critical axial strains obtained by present model and the results of Liew et al. (2004b) by using MD simulation for multi-walled CNTs of innermost radius $R_I = 0.34$ nm.

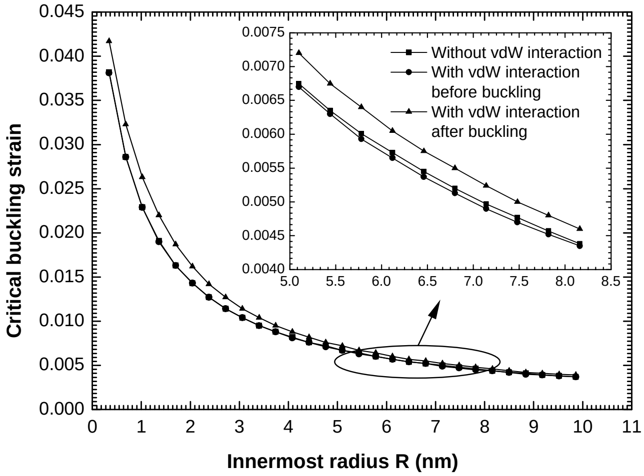

Fig. 6. Effect of the vdW interaction on the critical axial strain for a triple-walled CNT with various innermost radii.

radius is less than 7 nm, the critical strain descend very quickly with the increase of the innermost radius. However, when the radius is large enough, the critical strain decreases slowly as the innermost radius increases. It is observed that the critical axial strains with vdW interaction taken into consideration are higher than those without considering the vdW interaction, which coincide with the fact that the vdW interaction will raise the critical strain. This is because that when a tube deflects towards the other tubes, the vdW force generated is repulsive in nature. Whereas when a tube deflects away from the other tubes, the vdW force would be attractive in nature. Thus, the vdW interaction always has an effect against buckling and therefore vdW interaction will lead to an increase in the critical strain. Before the buckling, it is observed from Fig. 6 that the effect of vdW interaction on the critical strain is very small and can be neglected. In contrast, the influence of vdW interaction is significant after buckling for a triple-walled with small innermost radius. However, the effect of vdW interaction on the critical strain is negligible when the radius is large enough for both the cases of before and after buckling.

6. Conclusions

Explicit formulas are derived for predicting the critical axial strain of a triple-walled CNT, in which the more refined vdW model captures the effects of all layers, not just between two adjacent layers. Analyses of a cylindrical shell continuum model were carried out to investigate the vdW interaction between any two layers of a multi-walled CNT. The effect of the tube radius on the vdW interaction was also examined. Although we have considered a bifurcation buckling example, it should be noted that the more refined vdW model covers general infinitesimal deformation topics such as bending, torsion and even dynamics.

Ru (2000,2001) and Wang et al. (2003) reported that in the vdW interaction of adjacent layers of a multi-walled CNT, the vdW interaction coefficient c is not affected by the size of the tube. However, the results presented herein indicate a dependence of the vdW interaction on the radii of tubes.

The following conclusions can be drawn from the present study.

(1) The greatest contribution to the vdW interaction comes from the adjacent layers. The contribution from a remote layer is very little and can be neglected when the difference between the number of two layers is large enough, such as larger than 5.
(2) The vdW interaction is strongly dependent on the radius of the tube when the radius is small enough, such as less than 10 nm. When the radius is large enough, such as a radius larger than 40 nm, the coefficient c_{ij} can be considered as a constant.
(3) For the vdW interaction between different layers, the coefficient c_{ij} is different. For example when $n = 4$, for the interaction between adjacent nth and $(n-1)$th layers or nth and $(n+1)$th layers, the coefficient is -108 or -109 GPa/nm, as shown in Fig. 2a. For the interaction between nth and $(n-2)$th layers or nth and $(n+2)$th layers, the coefficient is 1.84 or 1.91 GPa/nm as shown in Fig. 2b. For the interaction between nth and $(n-3)$th layers or nth and $(n+3)$th layers, the coefficient is 0.167 or 0.171 GPa/nm, as shown in Fig. 2c.
(4) Before buckling, the effect of vdW interaction on the critical axial strain is very small and thus can be neglected. After buckling, the effect of vdW interaction on the critical axial strain is significant for a triple-walled CNT with small innermost radius. However, when the innermost radius is large enough, the influence of vdW interaction is also negligible.

References

Girifalco, L.A., 1991. Interaction potential for C_{60} molecules. Journal of Physical Chemistry 95, 5370–5371.

Girifalco, L.A., Lad, R.A., 1956. Energy of cohesion, compressibility, and the potential energy function of graphite system. Journal for Chemical Physics 25, 693–697.

Govindjee, S., Sackman, J.L., 1999. On the use of continuum mechanics to estimate the properties of nanotubes. Solid State Communications 110, 227–230.

Hernandez, E., Goze, C., Bernier, P., Rubio, A., 1998. Elastic properties of C and $B_xC_yN_z$ composite nanotubes. Physical Review Letters 80, 4502–4505.

He, X.Q., Kitipornchai, S., Liew, K.M., 2005. Buckling analysis of multi-walled carbon nanotubes: a continuum model accounting for van der Waals interaction. Journal of the Mechanics and Physics of Solid 53, 303–326.

Ijima, S., 1991. Helical microtubes of graphitic carbon. Nature 354, 56–58.

Ijima, S., Brabec, C., Maiti, A., Bernholc, J., 1996. Structural flexibility of carbon nanotubes. Journal of Chemical Physics 104, 2089–2092.

Kachanov, L.M., 1988. Delamination Buckling of Composite Materials. Kluwer Academic, Dordrecht.

Lennard-Jones, J.E., 1924. The determination of molecular fields: from the variation of the viscosity of a gas with temperature. Proceedings of the Royal Society 106A, 441.

Li, C., Chou, T.W., 2003a. A structural mechanics approach for the analysis of carbon nanotubes. International Journal of Solids and Structures 40, 2487–2499.

Li, C., Chou, T.W., 2003b. Elastic moduli of multi-walled carbon nanotubes and the effect of van der Waals forces. Composites Science and Technology 63, 1517–1524.

Liew, K.M., He, X.Q., Wong, C.H., 2004a. On the study of elastic and plastic properties of multi-walled carbon nanotubes under axial tension using molecular dynamics simulation. Acta Materialia 52, 2521–2527.

Liew, K.M., Wong, C.H., He, X.Q., Tan, M.J., Meguid, S.A., 2004b. Nanomechanics of single and multi-walled carbon nanotubes. Physical Review B 69, 115429.

Ru, C.Q., 2000a. Effective bending stiffness of carbon nanotubes. Physics Review B 62, 9973–9976.

Ru, C.Q., 2000b. Effect of van der Waals forces on axial buckling of a double-wall carbon nanotube. Journal of Applied Physics 87, 7227–7231.

Ru, C.Q., 2000c. Elastic buckling of single-walled carbon nanotube ropes under high pressure. Physics Review B 62, 10405–10408.

Ru, C.Q., 2001a. Axially compressed buckling of a double walled carbon nanotube embedded in an elastic medium. Journal of the Mechanics and Physics of Solids 49, 1265–1279.

Ru, C.Q., 2001b. Degraded axial buckling strain of multiwalled carbon nanotubes due to interlayer slips. Journal of Applied Physics 89 (6), 3426–3433.

Sanchez-Portal, D., et al., 1999. Ab initio structural, elastic, and vibrational properties of carbon nanotubes. Physical Review B 59, 12678–12688.

Saito, R., Matsuo, R., Kimura, T., Dresselhaus, G., Dresselhaus, M.S., 2001. Anomalous potential barrier of double-wall carbon nanotube. Chemical Physics Letters 348, 187–193.

Saito, R., Dresselhaus, G., Dresselhaus, M.S., 1998. Physical Properties of Carbon Nanotubes. Imperial College Press, London.

Timoshenko, S.P., Gere, J.M., 1961. Theory of Elastic Stability. McGraw-Hill, New York.

Wang, C.Y., Ru, C.Q., Mioduchowski, A., 2003. Axially compressed buckling of pressured multiwall carbon nanotubes. International Journal of Solids and Structures 40, 3893–3911.

Yakobson, B.I., Brabec, C.J., Bernholc, J., 1996. Nanomechanics of carbon tubes: instabilities beyond linear response. Physical Review Letters 76, 2511–2514.

Yakobson, B.I., Campbell, M.P., Brabec, C.J., Bernholc, J., 1997. High strain rate fracture and C-chain unraveling in carbon nanotubes. Computational Materials Science.

Yoon, J., Ru, C.Q., Mioduchowski, A., 2003. Vibration of an embedded multiwall carbon nanotube. Composite Science and Technology 63, 1533–1545.